arXiv:1207.4961v1 [cond-mat.quant-gas] 20 Jul 2012

Raman superradiance and spin lattice of ultracold atoms in optical cavities

Shabnam Safaei,[1, *] Özgur Esat Müstecaplıoğlu,[2] and B. Tanatar[1]
[1] *Department of Physics, Bilkent University, Bilkent, 06800 Ankara, Turkey*
[2] *Department of Physics, Koç University, Sarıyer, 34450 Istanbul, Turkey*

We investigate synthesis of a hyperfine spin lattice in an atomic Bose-Einstein condensate, with two hyperfine spin components, inside a one-dimensional driven high-finesse optical cavity, using off-resonant superradiant Raman scattering. Spatio-temporal evolution of the relative population of the hyperfine spin modes is examined by numerically solving the coupled cavity-condensate mean field equations in the dispersive regime. We find that beyond a certain threshold, depending on the transverse and parallel laser pumps and the atom-atom interactions, Raman superradiance and a self-organization of the hyperfine spin components simultaneously occur. Furthermore, the spin lattice can be made robust by ramping up the pump intensity in time then turning it off after a critical value.

PACS numbers: 37.30.+i, 42.65.Dr, 42.50.Pq, 37.10.Vz

An atomic gas inside a high-finesse optical cavity may exhibit self-organization when subject to transverse laser pump [1, 2]. In matter-cavity Quantum Electrodynamics (QED) systems, the mechanical effect of the electromagnetic fields on the motional states of atoms and phase shift effect of atomic motion on the fields induce each other mutually in a self-consistent loop. Developments in trapping of atomic Bose-Einstein Condensates (BEC) in high-finesse optical cavities [3–5] allow for sufficiently strong cavity-condensate coupling to realize nonlinear effects, such as bistability, even with cavity photon number below unity [6–8]. Quite recently, Dicke Superradiance (SR) quantum phase transition (QPT) [9–11] in a BEC-cavity system [12] has been demonstrated [13, 14].

Dicke QPT for the single-mode BEC inside a high-finesse cavity [13] is characterized by an abrupt increase in the number of cavity photons, after a certain threshold of the pump intensity, which is accompanied by broken translational symmetry of the condensate with the formation of an optical lattice [15]. Pump-cavity photon scattering couples the initial zero-momentum state of BEC to a superposition of higher recoil momentum states [16]. Quite a different scenario happens if a condensate of atoms with two different hyperfine sates is pumped by a laser field far-detuned from atomic transition [17, 18], in which case, Raman SR [19, 20] may occur during which the hyperfine state of atoms changes.

There has been much interest on multi-mode atom-cavity systems recently, such as bosonic Josephson junctions inside a single-mode cavity [21] and spin glasses of single-component BEC in a multi-mode cavity [22]. Optical bistability has been studied in spin-1 [23, 24] and in two-mode BECs [8, 25]. Multi-species systems provide a very rich platform for investigations of phase transitions, in addition to their practical advantages such as faster self-organization with lower threshold, [26] and efficient, easily interpretable imaging of correlations in phase transition by the cavity field [27, 28].

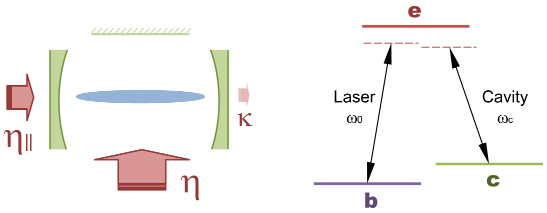

FIG. 1. (Color online) Left: Schematic drawing of a BEC in one dimensional optical cavity subject to parallel and transverse laser fields. Cavity has a decay rate of κ. Right: The doublet of lower levels (b and c) of the BEC atoms are coupled by cavity field and laser field via the atomic excited state e in Raman scattering scheme. Both laser field and cavity field are far detuned from the atomic transition frequencies.

We consider a condensate of N atoms with two non-degenerate hyperfine states, $|\,b\rangle, |\,c\rangle$ in a one dimensional single-mode cavity of frequency ω_c as shown in Fig. 1. The hyperfine states are coupled to an excited state $|\,e\rangle$ by a transverse pump of frequency ω_0 and the cavity field in Raman scheme. The cavity is driven by another laser with the same frequency ω_0. In the dispersive regime where the fields are far-detuned from the atomic transitions, the Hamiltonian of the system [19, 20] can be written as

$$
\begin{aligned}
H = &\sum_{j=b,c} \int dx\ \psi_j^\dagger \left(-\frac{\hbar^2}{2m}\frac{\partial^2}{\partial x^2} + V_j(x) + \hbar\omega_{bc}\delta_{j,c} \right) \psi_j \\
&+ \sum_{i,j=b,c} \int dx\ \frac{u_{ij}}{2} \psi_i^\dagger \psi_j^\dagger \psi_j \psi_i + H_{Raman} \\
&+ \hbar\omega_c a^\dagger a - i\hbar\eta_{||}(a e^{i\omega_0 t} - a^\dagger e^{-i\omega_0 t}), \qquad (1)
\end{aligned}
$$

where $\psi_j(x,t)$ ($\psi_j^\dagger(x,t)$) is the annihilation (creation) operator for a bosonic atom at space-time point (x,t). $V_j(x)$ is the external trap potential for the state $j = b, c, e$, ω_{bc} is the frequency of $b \leftrightarrow c$ transition and $\{u_{ij}\}$ are the interaction strengths of atoms in states i and j. The parallel laser field strength is denoted by $\eta_{||}$ and the annihilation (creation) operator of the cavity mode is a ($a^\dagger$).

For a cavity mode with wave number k, Raman scattering Hamiltonian (H_{Raman}) has the form

$$\begin{aligned} H_{Raman} = &-i\hbar \int dx\ \psi_e^\dagger h_0 (e^{-i\omega_0 t} + e^{i\omega_0 t})\psi_b + H.c. \\ &-i\hbar \int dx\ \psi_e^\dagger g_0 \cos(kx)(a + a^\dagger)\psi_c + H.c., \end{aligned} \tag{2}$$

where h_0 and g_0 are the atom-pump and atom-cavity dipole interaction strengths, respectively. Transverse pump profile is assumed to be wide enough to take h_0 uniform. Dipole approximation is used for the transverse direction. After adiabatically eliminating ψ_e, under the condition of $\Delta_0 = \omega_0 - \omega_{be}$ being larger than the excited state linewidth, the Hamiltonian reduces to

$$H = \sum_{j=b,c} \int dx\ \psi_j^\dagger \mathcal{H} \psi_j + \sum_{i,j=b,c} \int dx\ \frac{u_{ij}}{2} \psi_i^\dagger \psi_j^\dagger \psi_j \psi_i \tag{3}$$

where, in a rotating frame defined by the unitary operator $U = \exp -i\omega_0 t a^\dagger a$,

$$\begin{aligned} \mathcal{H} = &-\frac{\hbar^2}{2m}\frac{\partial^2}{\partial x^2} + \left(\frac{2\hbar h_0^2}{\Delta_0} + V_b(x)\right)\sigma^-\sigma^+ \\ &+ \left(\hbar U_0 \cos^2(kx)(aa^\dagger + a^\dagger a) + V_c(x) + \hbar\omega_{bc}\right)\sigma^+\sigma^- \\ &+ \hbar\eta(a + a^\dagger)\cos(kx)(\sigma^- + \sigma^+) \\ &- \hbar\delta_c a^\dagger a - i\hbar\eta_{||}(a - a^\dagger). \end{aligned} \tag{4}$$

Here $U_0 = g_0^2/\Delta_0$, $\eta = h_0 g_0/\Delta_0$, $\delta_c = \omega_0 - \omega_c$, $\sigma^+ = |c\rangle\langle b|$ and $\sigma^- = |b\rangle\langle c|$.

Early stages of the dynamics is strongly influenced by quantum fluctuations that triggers the SR. We consider the late time dynamics in which the condensate and field variables are assumed to be classical [20]. The effect of quantum fluctuations are introduced by seeding the cavity field in numerical simulations. In our case seeding is physically performed by the parallel pump that drives the cavity. The Heisenberg equations of motion in this mean-field regime take the following forms

$$\begin{aligned} \dot{\psi}_b = &-\frac{i}{\hbar}\left(-\frac{\hbar^2}{2m}\frac{\partial^2}{\partial x^2} + V_b(x) + \frac{2\hbar h_0^2}{\Delta_0}\right)\psi_b \\ &- \frac{i}{\hbar}\left(u_{bb}|\psi_b|^2 + u_{bc}|\psi_c|^2\right)\psi_b \\ &- 2i\eta\cos(kx)\alpha_r\psi_c \end{aligned} \tag{5}$$

$$\begin{aligned} \dot{\psi}_c = &-\frac{i}{\hbar}\left(-\frac{\hbar^2}{2m}\frac{\partial^2}{\partial x^2} + V_c(x) + \hbar\omega_{bc}\right)\psi_c \\ &- \frac{i}{\hbar}\left(2\hbar U_0\cos^2(kx)|\alpha|^2 + u_{cc}|\psi_c|^2 + u_{bc}|\psi_b|^2\right)\psi_c \\ &- 2i\eta\cos(kx)\alpha_r\psi_b \end{aligned} \tag{6}$$

$$\begin{aligned} \dot{\alpha} = &\, i\left(i\kappa + \delta_c - 2U_0\int dx\ |\psi_c|^2\cos^2(kx)\right)\alpha \\ &- i\eta\int dx\ \cos(kx)(\psi_c^*\psi_b + \psi_b^*\psi_c) + \eta_{||}, \end{aligned} \tag{7}$$

where α_r is the real part of the cavity field α and κ is the phenomenological decay rate of the cavity [20]. The Raman SR is identified by an abrupt increase in the number of cavity photons $n = |\alpha|^2$ while the QPT in the atomic system is monitored by the magnetization density $Z(x,t) = \frac{1}{N}(|\psi_b(x,t)|^2 - |\psi_c(x,t)|^2)$ which is normalized by the total number of atoms $N = \int dx(|\psi_b(x,t)|^2 + |\psi_c(x,t)|^2)$ so that the total magnetization Z can have extremum values 1 and -1 when all atoms are in mode b or c, respectively.

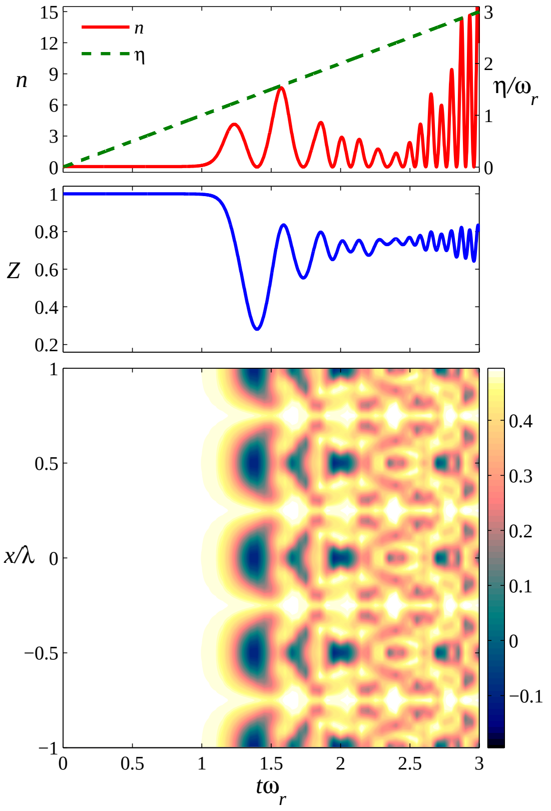

FIG. 2. (Color online) (top panel) Time dependence of strength of effective transverse laser pump η, dynamics of cavity photon number n, (middle panel) total magnetization Z, and (bottom panel) spatial and dynamical behavior of magnetization density $Z(x,t)$. Cavity photon number and magnetization indicate SR at which $Z(x,t)$ undergoes self-organization around the time $t \sim 1/\omega_r$. Magnetized and demagnetized domains are not well isolated. Here, in units of ω_r, $\eta_{||} = 1000$, $\omega_{bc} = 1$, $\kappa = 400$, $U_0 = -0.5$, $\delta_c = 4800$, $\Delta_0 = -4 \times 10^6$ and $N = 48 \times 10^3$.

Using second order split step method, and assuming all atoms are initially in hyperfine spin state $|\,b\rangle$, the mean field equations are solved numerically to monitor the dynamics of the system. Fig. 2 shows the time dependence of n (top panel) and Z (middle panel) as η increases in time scaled by the recoil frequency $\omega_r = \hbar k^2/2m$. Pump laser is considered to be red-detuned with $\Delta_0 < 0$, and thus $U_0, \eta < 0$. In all plots the absolute value of η is shown for convenience. Bottom panel of Fig. 2 demonstrates the spatio-temporal dynamics of magnetization density, where its translational symmetry is broken at the threshold of Raman SR. We consider a condensate of length 2λ, λ being the wavelength of the cavity mode, and hence initially $Z(x, t = 0) = 0.5$. At the SR threshold, atoms change their internal states by Raman scattering of the transverse pump into the cavity field. However not all atoms can equally contribute due to spatial modulation of the Raman coupling by the cavity mode. Raman couplings in (5) and (6) change both the hyperfine spin and the motional states of the atoms. The recoil momentum of the atoms changes by $\pm\hbar k$. Atoms in in state $\mid c\rangle$ cause a shift in the cavity resonance due to their spatial overlap with the cavity mode by $-2U_0 \int dx\ |\psi_c|^2 \cos^2(kx)$. The cavity mode builds a standing wave potential, $2\hbar U_0 \cos^2(kx)|\alpha|^2$, whose minima traps the atoms in $\mid c\rangle$ at $x_j = j\lambda/2$ where j is an integer. Overlap of different hyperfine spin states act as an atomic polarization grating which is enhanced around the sites x_j and stimulates even more Raman scattering that completes a self-consistency loop. Accumulation of the atoms in $\mid c\rangle$ around the sites x_j while the atoms in $\mid b\rangle$ around the nodes of the cavity mode, which are protected from Raman interactions, results in a spatial distillation of the atoms in different hyperfine spin states, manifested as a self-organized magnetic lattice with a lattice constant $\lambda/2$. Fig. 2 reveals that magnetized domains are not well isolated from the de-magnetized ones and there is no robust pseudospin lattice structure due to too many ringing of the SR pulse.

We can envision a simple scenario where a robust lattice of well isolated pseudospin domains can be obtained if we just turn the transverse pump off once the magnetization reaches its first minimum. This happens when $\eta = 1.4\ \omega_r$. Fig. 3 shows the dynamics of n, Z and $Z(x,t)$ for the case where η increases from 0 to 1.4 ω_r and then is abruptly turned off. Parallel laser pump remains on but has no effect. Due to the lack of Raman coupling, magnetization Z remains constant after switching the transverse field off.

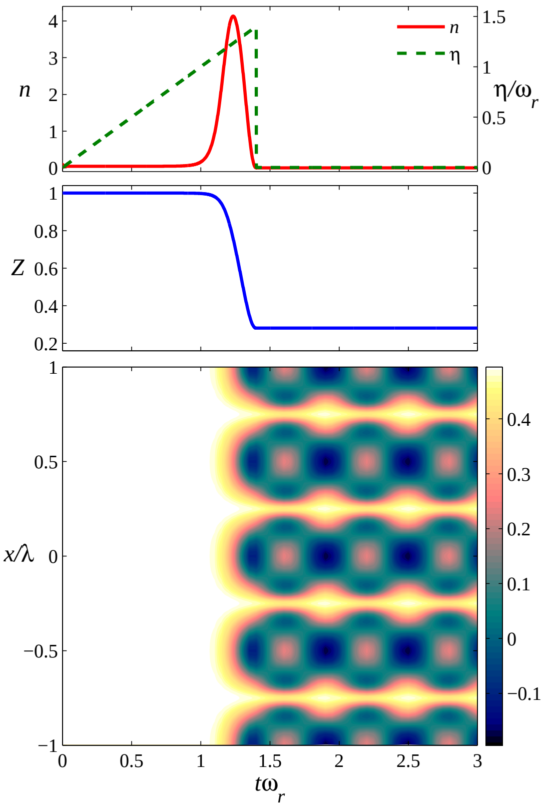

FIG. 3. (Color online) Dynamics of cavity photon number n (top panel), magnetization Z (middle panel) and magnetization density $Z(x,t)$ (bottom panel) as the intensity of transverse laser field η is increased from 0 to 1.4 ω_r and then is switched off. Other parameters are the same as Fig. 2. Here, the magnetized domains are well isolated by the de-magnetized ones, and a robust magnetic lattice is synthesized.

Finally we briefly discuss the effect of the interactions and the parallel pump on the threshold of Raman SR. Presence of a parallel laser pump plays the role of usual seeding of superradiant modes in the numerical mean field treatment of the SR in the late time classical regime. The critical strength of transverse pump η_c for Raman SR to happen is numerically determined when Z starts dropping significantly after crossing $Z = 0.98$. Top panels of Fig. 4 indicate that significant increase of the parallel laser pump strength would reduce, albeit slightly, η_c, but further increase of $\eta_{||}$ would not yield to smaller values of η_c. In Fig. 4 right panels present the same data as in left panels but in logarithmic scale. In the presence of atom-atom interactions, the system reaches superradiant phase faster and at a lower threshold as the comparison of top and bottom panels of Fig. 4 reveals. Bottom panels are without the interactions. The interaction coefficients $u_{ij} = 4\pi\hbar^2 a_{ij}/m$ are calculated with the s-wave scattering lengths $\{a_{ij}\}$ taken to be $a_{bc} = a_{cb} = 90$ a.u. $\approx 5.95 \times 10^{-3}\ \lambda$ and $a_{bb} = a_{cc} = 106$ a.u. $\approx 7.01 \times 10^{-3}\ \lambda$, with $\lambda = 800$ nm. This analysis verifies that the parallel pump contributes weakly to the threshold of Raman SR.

We conclude that a BEC with two non-degenerate hyperfine spin components in a high-finesse cavity driven by transverse and parallel pumps can exhibit Raman SR above a critical value of transverse field strength. Simultaneously, BEC undergoes a phase transition, associated both with the external and internal degrees of freedom, during which atoms scatter transverse laser field into the cavity mode and in return their hyperfine state changes. As a result, cavity photon number rises abruptly and at the same time there is a sudden increase in the population of higher hyperfine state at periodical positions. Self-organization yields spatial distillation of atoms in different hyperfine states exhibiting a magnetic lattice configuration.

Even though present analysis is in the mean field regime, we can envision that hyperfine spins at different lattice sites would be entangled as they interact with the

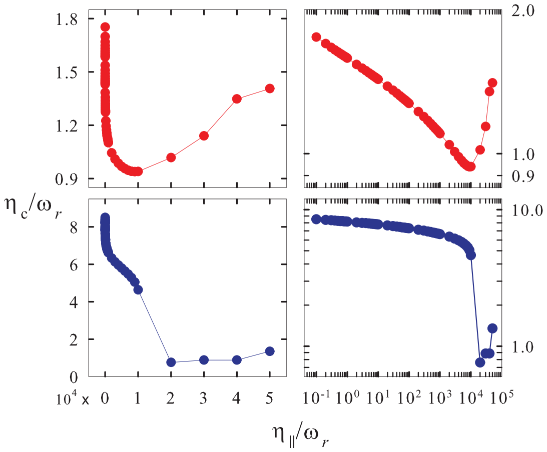

FIG. 4. (Color online) Numerically-obtained critical transverse laser strength η_c as a function of the strength of parallel laser $\eta_{||}$, for the cases with (top panels) and without (bottom panels) atom-atom interaction. Right panels show same data as left panels in logarithmic scale. Atomic scattering lengths are given in the text and other parameters are the same as Fig. 2.

common cavity field, following the resonant entanglement of atoms in multitraps scenario [29]. Availability of large number of spins per site could make the system advantageous for explorations of magnetic supersolid properties. In contrast to Rayleigh SR, Raman SR can be used for a source of entangled photon-spin pairs. Synthesis and probing lattice spin models in a single compact cavity design, with fast SR induced QPT and self-organization properties, promise unique opportunities for quantum information applications as well as monitoring QPTs and spin correlations with Raman scheme.

This work was supported by TÜBİTAK (Grant. No. 109T267).

---

* safaei@fen.bilkent.edu.tr

[1] P. Domokos and H. Ritsch, Phys. Rev. Lett. **89**, 253003 (2002).
[2] A. T. Black, H. W. Chan, and V. Vuletić, Phys. Rev. Lett. **91**, 203001 (2003).
[3] P. Horak, S. M. Barnett, and H. Ritsch, Phys. Rev. A **61**, 033609 (2000).
[4] F. Brennecke, T. Donner, S. Ritter, T. Bourdel, M. Köhl, and T. Esslinger, Nature **450**, 268 (2007).
[5] Y. Colombe, T. Steinmetz, G. Dubois, F. Linke, D. Hunger, and J. Reichel, Nature **450**, 272 (2007).
[6] S. Gupta, K. L. Moore, K. W. Murch, and D. M. Stamper-Kurn, Phys. Rev. Lett. **99**, 213601 (2007).
[7] S. Ritter, F. Brennecke, K. Baumann, T. Donner, C. Guerlin, and T. Esslinger, App. Phys. B **95**, 213 (2009).
[8] S. Safaei, Ö. E. Müstecaplıoğlu, and B. Tanatar, arXive:1207.1858 (2012).
[9] R. H. Dicke, Phys. Rev. **93**, 99 (1954).
[10] K. Hepp and E. H. Lieb, Ann. Phys. **76**, 360 (1973).
[11] Y. K. Wang and F. T. Hioe, Phys. Rev. A **7**, 831 (1973).
[12] D. Nagy, G. Kónya, G. Szirmai, and P. Domokos, Phys. Rev. Lett. **104**, 130401 (2010).
[13] K. Baumann, C. Guerlin, F. Brennecke, and T. Esslinger, Nature **464**, 1301 (2010).
[14] K. Baumann, R. Mottl, F. Brennecke, and T. Esslinger Phys. Rev. Lett. **107**, 140402 (2011).
[15] V. I. Yukalov, Laser Phys. **19**, 1 (2009).
[16] M. J. Bhaseen, J. Mayoh, B. D. Simons, and J. Keeling, Phys. Rev. A **85**, 013817 (2012).
[17] D. Schneble, G. K. Campbell, E. W. Streed, M. Boyd, D. E. Pritchard, and W. Ketterle, Phys. Rev. A **69**, 041601(R) (2004).
[18] Y. Yoshikawa, T. Sugiura, Y. Torii, and T. Kuga, Phys. Rev. A **69**, 041603(R) (2004).
[19] M. M. Cola ande N. Piovella, Phys. Rev. A **70**, 045601 (2004).
[20] H. Uys and P. Meystre, Phys. Rev. A **75**, 033805 (2007).
[21] J.-S. Huang, Z.-W. Xie, and L.-F. Wei, Commun. Theor. Phys. **55**, 59 (2011).
[22] P. Strack and S. Sachdev, Phys. Rev. Lett. **107**, 277202 (2011).
[23] L. Zhou, H. Pu, H. Y. Ling, and W. Zhang, Phys. Rev. Lett. **103**, 160403 (2009).
[24] L. Zhou, H. Pu, H. Y. Ling, K. Zhang, and W. Zhang, Phys. Rev. A **81**, 063641 (2010).
[25] Y. Dong, J. Ye, and H. Pu, Phys. Rev. A **83**, 031608(R) (2011).
[26] T. Griesser, W. Niedenzu, and H. Ritsch, New J. Phys. **14**, 053031 (2012).
[27] L. Guo, S. Chen, B. Frigan, L. You, and Y. Zhang, Phys. Rev. A **79**, 013630 (2009).
[28] B. Öztop, M. Bordyuh, Ö. E. Müstecaplıoğlu, and H. E. Türeci, arXiv:1107.3108 (2011).
[29] V. I. Yukalov and E. P. Yukalova, Phys. Rev. A **73**, 022335 (2006).